Regional Studies in Marine Science 89 (2025) 104290

Contents lists available at ScienceDirect

Regional Studies in Marine Science

journal homepage: www.elsevier.com/locate/rsma

Shallow gas seeps offshore Crimea (Black Sea): Mapping, bubble flow quantification and geochemical study

T.V. Malakhova [a,b,*], M.M. Makarov [c], A.I. Khurchak [a], A.P. Stetsiuk [a], K.M. Kucher [c], N.S. Syrbu [d], A.A. Legkodimov [d], M.V. Ivanov [d], A.A. Budnikov [e]

[a] A.O. Kovalevsky Institute of Biology of the Southern Seas of RAS, Sevastopol, Russia
[b] International Research Center for Ecology and Climate Change, Sirius University of Science and Technology, Sochi, Russia
[c] Limnological Institute SB RAS, Irkutsk 664033, Russia
[d] V.I. Il'ichev Pacific Oceanological Institute FEB RAS, Vladivostok 690041, Russia
[e] Lomonosov Moscow State University, Leninskie Gory, 1, Moscow 119991, Russia

ARTICLE INFO

Keywords:
Shallow methane seep
Hydroacoustic surveys
Gas flow
Mercury
Black Sea

ABSTRACT

This paper is the first focused study of gas bubble emissions at the Crimean shelf in the northern Black Sea. During R/V Professor Vodianickiy 125/1 Cruise in November 2022 hydroacoustic and geochemical studies were carried out to detect gas seepage along Crimean coastline to assess methane-related processes taking place in the local hydrosphere. More than 200 bubble-induced hydroacoustic anomalies in the water column were found at 7.1 km^2. We allocated 4 seepage areas which are arranged in the west of the study area and included most of the identified flares located primarily along 35 – 45 m isobaths. Vertical profiles of temperature, salinity, dissolved oxygen content were measured, and a video survey of the seafloor was conducted. The spatial and temporal variability of the flares was examined at Martyan seep site by multiple hydroacoustic surveys on a hours- and days-scales. The observations of the flare appearance showed that most flares are temporally variable. Calculated gas flow rate from individual flare ranged from 4.1 (0.04) to 88.6 (0.101) $L\cdot day^{-1}$ ($t\cdot year^{-1}$), while the average value was 38 (0.07) $L\cdot day^{-1}$ ($t\cdot year^{-1}$). Distinct methane transport from the seep sites into the hydrosphere was observed only for Martyan seep area by relative enrichments of dissolved methane in near-bottom waters. Sediments from the active seep area were significantly enriched in mercury (87 ± 21 ng g^{-1}) compared to the reference sites (26 ± 7 ng g^{-1}). Our analyses provide one of the first interdisciplinary descriptions of shallow gas seeps sites within the Black Sea seep system.

1. Introduction

Methane is a key climate-relevant trace gas, widely encountered in seawater (Reeburgh, 2007; Weber et al., 2019). Considerable research efforts have been made to comprehend its sources and sinks (Intergovernmental Panel on Climate Change (IPCC), 2023). Cold seeps are predominantly methane bubbles and fluid gas migration from the sedimentary subsurface to the seabed and into the water column. With the potential for some methane to eventually reach the atmosphere, it is crucial to monitor its emissions to assess environmental impact (McGinnis et al.,2006; Suess, 2014; Ceramicola et al., 2018). Accurate quantification of methane flux at hydrocarbon seeps is necessary to evaluate their influence on the global methane budget and climate change (Kvenvolden and Rogers, 2005; Saunois et al., 2020) as well as to assess its role as a material and energy source that contributes to food chains in various aquatic environments (Baumberger et al., 2022).

As of approximately 10 years after the first discovery of submarine hydrocarbon seep systems in the 1980s, a number of hydrocarbon seep sites have been found also in the Black Sea. The presence of cold seeps here was first confirmed hydroacoustically in April 1989 during the 28th Cruise of RV Professor Vodianickii (Egorov et al., 2011). To date, the questions related to cold methane seeps in the Black Sea have been already discussed in books about global seabed fluid flow (Judd and Hovland, 2009), mineral resources of the Black Sea (Shnyukov and Ziborov, 2004), as well as in fundamental work on the study of the biogeochemical cycle of methane in the ocean (Lein and Ivanov M. V., 2009).

More than two decades ago, Egorov et al., (2011) published an

* Corresponding author at: A.O. Kovalevsky Institute of Biology of the Southern Seas of RAS, Sevastopol, Russia.
E-mail address: t.malakhova@ibss-ras.ru (T.V. Malakhova).

https://doi.org/10.1016/j.rsma.2025.104290
Received 18 October 2024; Received in revised form 7 April 2025; Accepted 5 June 2025
Available online 6 June 2025
2352-4855/

analysis and associated database for > 4000 water column methane seeps discovered since 1989 in the Black Sea. The seeps database published with Egorov et al. (2011) relied on echosounder surveys during 23 scientific cruises by research vessels between 1992 and 2005. Furthermore Egorov et al. (2011) analyzed the state of the art of Black Sea cold seeps impact on the hydrochemical and hydrological characteristics of the marine environment, as well as bioecological aspects of gas emissions. Egorov et al. (2011) proposed a model for gas exchange between bubbles and water column and assessed methane emission from gas seeps to the water and atmosphere.

In the intervening decades, numerous studies have significantly enhanced the understanding of the Black Sea hydrocarbon seeps, e.g., possible sea-air methane exchange (Amouroux et al., 2002); the fate of emitted methane in the water column (Ivanov et al., 2002); the characteristics of seep benthic communities and methane-derived carbonates (Novikova et al., 2015). Some sites have become model systems for understanding the variability of hydrocarbon seepage and associated biogeochemical processes. High-intensity gas releases have been described at the Dnepr paleo-fan (Naudts et al., 2006; Schmale et al., 2010), Don-Kuban paleo-fan (Starostenko et al., 2010) and Danube fans (Hillman et al., 2018; Riedel et al., 2021), at the Caucasian gas seep area (Pape et al., 2011; Körber et al.,2014; Pape et al., 2021) and Turkish gas seep area (Akhmetzhanov et al., 2007; Özel et al.,2022). Thus during the three decades, the Black Sea has become one of the areas in the world with the most intensive studies on hydrocarbon seep systems. However, much less attention has been paid to shallow coastal areas, which are important in the context of methane contribution to the atmosphere (Judd and Hovland, 2009).

Among the inland seas, the Black Sea is one of the largest meromictic and methane reservoir; many works have been devoted to the study its methane biogeochemistry (Lein et al., 2009; Egorov et al., 2011). The methane concentration in the surface layer is 1– 10 nmol L^{-1}, increasing more than 1000 times in anoxic zone to 11–12 μmol L^{-1} (Lein et al., 2009). Vast anoxic zone with an extremely high dissolved methane content has formed under the Black Sea pycnocline, located at a depth of more than 100 m. Schmale et al. (2005) concluded that only shallow seeps (depths <100 m) seem to affect the methane concentration of surface water and direct local emissions into the atmosphere, while

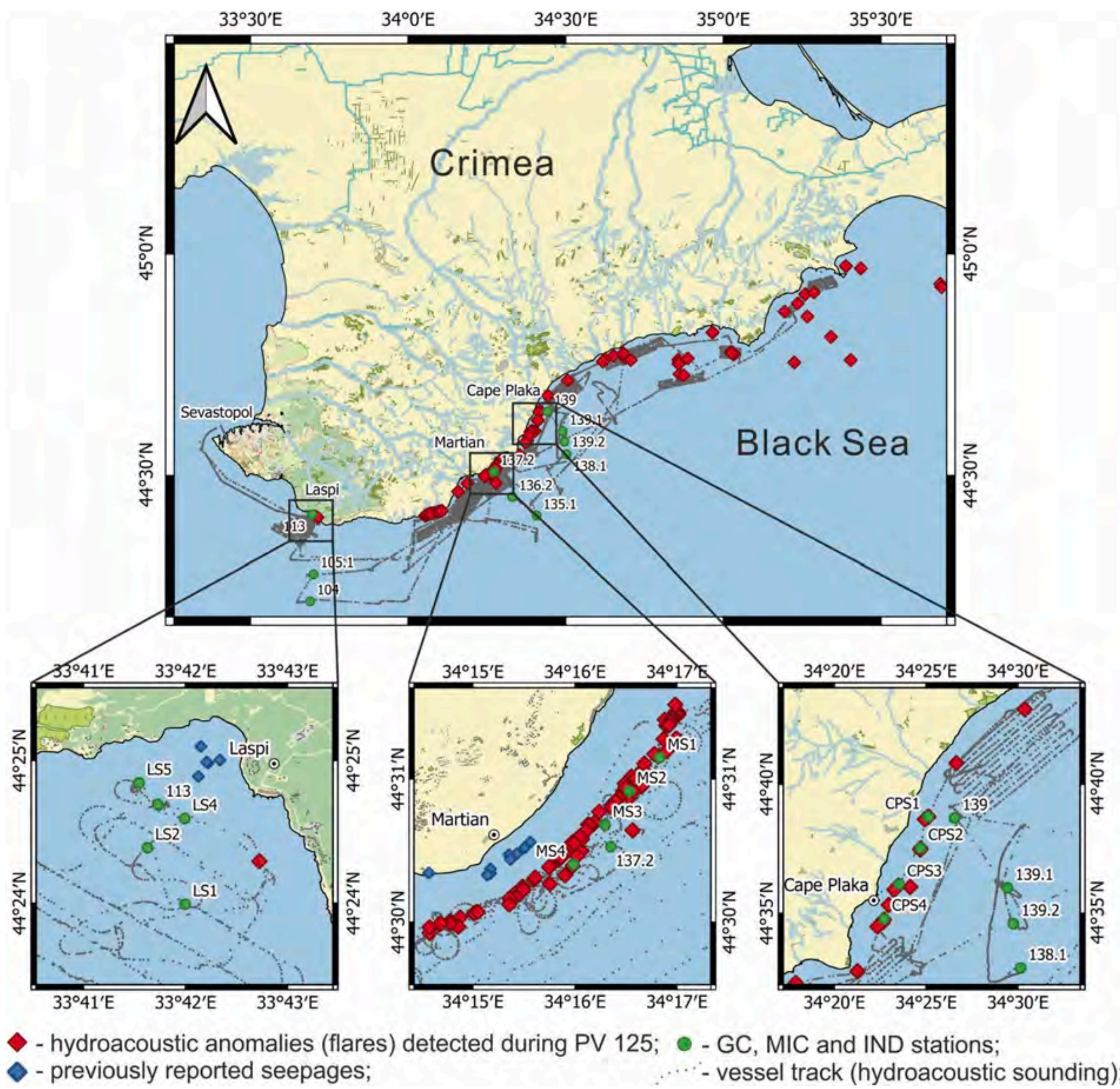

Fig. 1. Map of the study area at southern Crimean continental margin of the Black Sea showing ship-track and about 200 hydroacoustic anomalies (flares) indicative for ascending gas bubbles in the water column, as well as GC and MIC sample stations (Table 1). Flares cluster in 3 distinct areas (Laspi, Martyan and Cape Plaka seep sites) are shown in the boxes below.

high-intensity seep sites below this boundary do not show regional influence on the surface layer. Greinert et al. (2010) highlighted how methane fluxes rapidly increase with increasing bubble size and decreasing water depth, underlining that shallow sites may represent a significant source of methane to the atmosphere. Even in shallow locations, vertical transport can be restricted by density stratification. Therefore, the study of shallow-water methane seeps is important in the context of the global climate agenda.

Very shallow-water methane seepages have been reported by now near south coast of Crimean peninsula (Malakhova et al., 2010; Tarnovetskii et al., 2018 Budnikov et al., 2019; Malakhova et al., 2020, 2020; Malakhova et al., 2023a, 2023b. However, previous surveys have been limited to specific areas of work and have been conducted from shore by divers or small vessels. During 125/1 cruise by R/V Professor Vodianickiy in November 2022 we performed a hydroacoustic survey and visual seafloor observation to detect gas seepage along coastline as well as hydrochemical analysis in the sediments and water column to assess methane-related processes taking place in the local hydrosphere.

2. Regional setting

2.1. Geological settings

Study area is located on the Crimean shelf in the Black Sea (Fig. 1), which is characterized by shallow water depth. The shelf and continental slope (continental terrace) of the Crimean Peninsula within the Black Sea can be divided into three morphostructural regions: Western, from Tarkhankut to the Bay of Laspi and Cape Sarich; Southern coast, from Cape Sarich to Cape Meganom; Eastern, including the area of Feodosiya Bay and the Kerch-Taman shelf. The narrow shelf along the southern coast of Crimea is submerged, albeit to a lesser extent. East of Cape Meganom, the shelf widens, with the depth at the outer edge ranging from 100 to 130 m. Throughout the shelf of the Crimean Peninsula, there are internal, abrasion, and accumulative outer parts. The boundary between them lies at 80–95 m. The abrasion plain of the inner shelf is overlain by a sedimentary cover of small thickness (10–20 m), mainly of late-Neoeuxinic to Holocene age. The accumulative layer of the outer shelf is represented by a clinoform, which apparently formed mainly during post-Karangat times under regressive conditions. Below the upper clinoform, seismic-acoustic studies have identified three similar formations, and deltaic accumulation may have started as early as the Pliocene (Sheremet et al., 2016). Sea level fluctuations have stimulated gravitational processes on the continental slope. The alluvial cone opposite the Yalta amphitheater represents a large sedimentary body among other similar formations - alluvial cones of the pre-Kuban, pre-Don, and other rivers. The absence of a major river on the southern coast of Crimea could have been partially compensated by increased flow from karst springs of the Main Ridge during glacial epochs with their pluvial conditions.

2.2. Very shallow hydrocarbon seeps in the Crimean shelf area

Previous studies indicate very shallow gas seepages distributed at separate sites (Tarnovetskii et al., 2018; Budnikov et al., 2019; Malakhova et al., 2020; Malakhova et al., 2023a; Malakhova et al., 2023b. This researches focused mostly on 3 gas seeps areas (Laspi, Sevastopol and Cape Tarkhankut seep areas) while much less attention is paid to gas emission areas in other shallow regions. Crimean coastal seeps were mostly of biogenic origin, with a seasonal type of gas bubble emission (Malakhova et al., 2020). A significant variation was recorded in values of isotopic composition of methane carbon $\delta^{13}C\text{-}CH_4$ of bubble gas in coastal shallow areas (−94…−34 ‰), which indicates different conditions for bubble gas generation and maturation in seabed sediments (Malakhova et al., 2020a, 2020b). Various methods were used to estimate the size spectra of bubbles, as well as fluxes from separate seeps. Gas flux values varied from 1.8 L·day^{-1} (the Martynova Bay, Malakhova T. V., 2010) to 40 L·day^{-1} (the Laspi Bay, Malakhova et al., 2020a, 2020b).

3. Materials and methods

All data used in this study were collected during 125/1 cruise RV “Professor Vodianickii” (PV125/1) was conducted during 2–26 November 2022.

- GC - non-pressurized sediment cores
- IDR - IDRONAUTOCEANSEVEN 320 PlusM;
- TUV - teleoperated underwater vehicle «ROVBUILDER»
- MIC - mini corers;

3.1. Hydroacoustic methods

Hydroacoustic survey was carried out using the hydroacoustic complex “Echo-Baikal”, which is a software-hardware complex of the upgraded Furuno FCV-1100 echo sounder (Japan) and proprietary software. The complex was configured for dual-frequency mode with the parameters: zonding signal frequency 50 and 88 kHz, pulse duration 0.2 ms, noise level treshold −142 dB. The directional pattern characteristic of transducers at a level of −3 dB for 50 and 88 kHz were 8 and 7 deg, respectively. The transducers of the R/V “Professor Vodyanitsky” installed into the vessel bottom were used. The hydroacoustic complex was calibrated using a standard method (Simrad) using a copper sphere with a diameter of 60 mm a target strength (TS_50kHz) value of −38.59 dB.

3.2. Calculation of bubble gas flows (estimation from size spectra)

Algorithm was similar to the model presented in Veloso et al. (2015). Briefly, the available information obtained from the echosounder is given in terms of target strength (TS) which is the logarithmic version of the total backscattering cross-section. TS is calculated for each sample of each ping and therefore each TS value represents the backscattering produced by the targets located at the approximated truncated conical volume with a depth given by the time sample interval of the received signal.

The model simulates a combination of bubbles within a sample volume that aligns with the Bubble Size Distribution (BSD) and the measured total acoustic scattering cross-section. For calculation of bubble gas flows we make a number of assumptions. 1. We estimate the gas flow at the bottom-water boundary (so-called “initial flow”). Thus, we avoid answering how much gas has dissolved in the water and how much gas has reached the sea surface. 2. To calculate the total volume of gas in bubbles, we use BSD obtained from video recordings of shallow gas seeps in the Black Sea (see Fig, S1. in supplement). 3. We also assume that the bubbles are filled with methane only, so the gas density, heat capacity ratio, acoustic damping coefficient, and other characteristics are calculated for this gas only.

Post-processing for calculating gas flow is based on the “Echo-Baikal” software and a self-written MATLAB based software package, which calculates target strength TS and backscattering volume strength SV (Muyakshin and Sauter, 2010; Makarov et al., 2020). Taking into account the parameters of the external environment - depth, temperature, pressure and water density and the above-mentioned assumptions, a single gas bubble at the depth of the bottom-water boundary is modeled and its acoustic cross-section is calculated. The number of bubbles is increased until their total acoustic cross-section in terms of target force exceeds TS measured by the echo sounder. As a result, we obtain the number of bubbles and their total gas volume, as well as their mass. Knowing the size of bubbles, using the A.Liefe equation, we calculate the bubble ensemble surfacing velocity and gas flow rate (volumetric, mass, molar) for a particular gas outlet, as presented in (Makarov et al., 2020;

Muyakshin and Sauter, 2010).

3.3. Water column analyses

To identify the size and magnitude of the dissolved methane plume generated by the bubble discharge, seawater was sampled along a hydrocast transects that crossed the active gas emission sites (Table 1, Fig. 1). The transects extend about 1 km along the coastline and each include 4 stations. We used a rosette equipped with 12 5-L Niskin bottles mounted on a frame that holds a IDRONAUT OCEANSEVEN 320 PlusM plus conductivity, temperature, depth, oxygen sensors. For quantification of methane concentrations in the water column 30 mL of sampled seawater were transferred from the Niskin bottles into glassbottles immediately after recovery (see 3.6. for gas chemical composition analytical procedure).

3.4. Sediment sampling

Non-pressurized sediment cores were recovered with gravity corers occasionally lined with PVC-liner (GC; 3 m core length) and mini corers (MIC; <0.5 m). In total, 10 GC and 4 MIC cores of sediments were investigated (Table 1). Sediments were subsampled from GC in 20–40 cm-resolution on deck, MICs were transferred immediately upon recovery into the cold room and sampled in 5–10 cm resolution.

For vertical profiling of methane concentrations in GC and MIC sediments, a modified headspace technique was used. 2,5 milliliter of sediment were taken with cut-off syringes immediately after core recovery, when concentrations of light hydrocarbons have still not equilibrated to atmospheric pressure, at defined depths and transferred into 25 mL glass vials prefilled with NaOH. The samples were stored at 4 °C until analysis onshore.

3.5. Hydrological data (RCM 9 LW)

At Martyan seep area RCM 9 LW (AANDERAA, Norway) multi-sensor meter was used in a bottom frame mooring on November 15 (44°30.463 N, 34°15.871 E) and November 23, 2022 (44°31.185 N, 34°16.856 E). The depth at the site was 44 m. The measured parameters were temperature T (here and after sensor accuracy/resolution ±0.05/ 0.03∘C), conductivity C (±0.018 mS cm−1/ 0.002 mS cm−1), dissolved oxygen concentration DO (<8 μmol/L /<1 μmol/L), turbidity Tu (±10/ 0.5 NTU), current speed (0.3 cm/s/0.3 cm/s), current direction (±5∘/ 0.35∘). The recording goes on continuously. One recording interval takes 34 s. Water salinity was calculated from measured temperature T and electrical conductivity Cк using formulas from the paper (Zori et al., 2000).

3.6. Gas chemical composition

3.6.1. 3.6.1. CH4 и C2 +

A static headspace-equilibrium method was adopted for the CH_4 measurements (Kolb, 2006). A 4-mL helium (99.9999 %, mark 5.0, LLC "Argon", Russia) headspace was created inside the vial with a gas-tight syringe. The samples were vibrated and then left to reach the CH_4 equilibrium between air and water phases. 250-μL subsamples of headspace gas were injected into a gas chromatograph equipped with a flame ionization detector (GC-FID, Hewlett-Packard 5890 Series II, Agilent Technologies, Santa Clara, CA, USA and in the Scientific and Educational Center for Collective Use "Spectrometry and Chromatography" of the IBSS using a Kristall 5000 gas chromatograph (Khromatek, Russia)). Compound separation was achieved with a packed column (1 m length, inner diameter 2 mm, Porapack Q 80/100 mesh, Serva) under the following conditions: the carrier gas was nitrogen, flow rate – 30 mL/min, temperature of the detector – 225 °C and of the injector –120 °C. Standard gas mixtures with varying mole fractions of CH_4 in nitrogen ("Monitoring", St. Petersburg, Russia) were used daily to calibrate the response of FID before measurements. Relative standard deviations on measurements obtained under field conditions were 7 %.

3.6.2. Helium

For helium analysis, gas chromatograph "Chromatec-Gazochrom 2000" (JSC "Chromatec", Yoshkar-Ola) with high-sensitivity thermal conductivity sensors was used. The carrier gas was argon. Certified calibration gas mixtures were used to calibrate the instruments. The error of this method is less than 5 %. Identification of helium and hydrogen in bottom sediments was carried out using the method of equilibrium concentrations (Obzhirov, 1993; Wiesenburg and Guinasso Jr, 1979).

3.7. Hg

Mercury concentrations were detected in 11 cores (123 bottom

Table 1
List of stations investigated at Crimean continental margin during PV125/1.

Area	Sample code	Instrument type	Data	Depth, m	Coordinates	
Laspi seep area	113	GC, IDR, TUV	03.11.2022	53	44°24.692	33°41.729
	105,1	GC, IDR	16.11.2022	118	44°16.620	33°42.023
	104	GC, IDR	16.11.2022	145	44°12.922	33°41.362
	LS1	MIC, IDR	25.11.2022	66	44°23.995	33°41.995
	LS2	IDR	25.11.2022	63	44°24.389	33°41.626
	LS4	MIC, IDR	25.11.2022	50	44°24.594	33°41.992
	LS5	IDR, TUV	25.11.2022	-	44°24.843	33°43.544
Martyan seep area	137.2	GC, IDR, TUV	04.11.2022	55	44°30.528	34°16.351
	136.2	GC, IDR	14.11.2022	700	44°27.092	34°19.812
	135.1	GC, IDR	14.11.2022	1119	44°24.546	34°24.445
	MS1	MIC, IDR	24.11.2022	51	44°31.150	34°16.829
	MS2	IDR	24.11.2022	44	44°30.915	34°16.529
	MS3	IDR	24.11.2022	44	44°30.679	34°16.294
	MS4	IDR	24.11.2022	46	44°30.404	34°15.983
Cape Plaka seep area	139.1	GC, IDR	13.11.2022	130	44°35.991	34°29.424
	139	GC, IDR		65	44°38.692	34°26.534
	139.2	GC, IDR		580	44°34.596	34°29.746
	138.1	GC, IDR		1300	44°32.885	34°30.140
	CPS1	MIC, IDR, TUV	23.11.2022	35	44°38.741	34°25.101
	CPS2	IDR	23.11.2022	43	44°37.532	34°24.693
	CPS3	IDR	24.11.2022	39	44°36.132	34°23.525
	CPS4	IDR	24.11.2022	51	44°34.793	34°22.705
Megaseep	MegaS	GC, IDR, TUV	21.11.2022	40	44°46.548	34°40.938

sediments samples). To determine mercury, an RA-915M+ mercury analyzer with a PYRO-915 pyrolytic attachment was used. The lower detection limit was 0.5 ng g^{-1}. The analysis error was 2–3 %. GSO 7183–95, SPDS-1,2,3, HISS-1, MESS-4, and PACS-3 served as reference materials for mercury. External control was carried out annually in the manufacturer's laboratory (Lumex LLC, St. Petersburg).

3.8. Visual Seafloor observations

The Rovbuilder RB 300 (Russia), a towed underwater system equipped with a high-resolution digital camera, was used to visually inspect the sea floor at an altitude of about 1.5–2 m relative to the seabed in areas where flares were detected using echosounder. In addition to the provided live feed, the camera was programmed to take high-resolution photographs of the sea floor for target-objects.

4. Results

4.1. Seep locations

During hydroacoustic surveys anomalies in the water column (gas flares) diagnostic for gas bubble release from the seafloor were observed on the Crimean continental margin using the Furuno and Simrad echosounder (see Table S1. in supplement materials for a full list of seeps).

The seeps were composed of vertically arranged oblique reflections that image the up-rising individual bubbles or groups of bubbles (Fig. 2). In total, more than 200 individual seeps were detected in the 7,1 km^2 area during our study (Fig. 1, Table S1). These seeps were originating at seafloor depths between 19,7 and 78,5 m below sea level (mbsl) and are preferentially located at the closest transect to the shore (Fig. 3, Table S1). The seeps showed mostly vertical orientation and were about 20 m high. It is difficult to determine the real height of the seeps due to the narrow directional pattern of transducer (6° for Furuno 50 kHz, 7° for Simrad EK500 120 kHz). Such a small angle results in loss of the uppermost part of the seeps in the beam when the ship did not pass exactly through the center of the bubble train. Some seeps detected were discontinuous or were disconnected from the sea floor.

One of the steps in analysing seep dataset was identifying seep clusters, defined as groups of seeps that are close enough together. We allocated 4 seep clusters (Alupka, Martyan, Cape Plaka and Ribach'e) which are arranged in the west of the study area and included most of the identified hydroacoustic anomalies. Most of the gas flares were fixed near Cape Martyan, mainly along the isobath with a depth of 35–45 m (Fig. 3). In the eastern part of the study area were mostly individual flares.

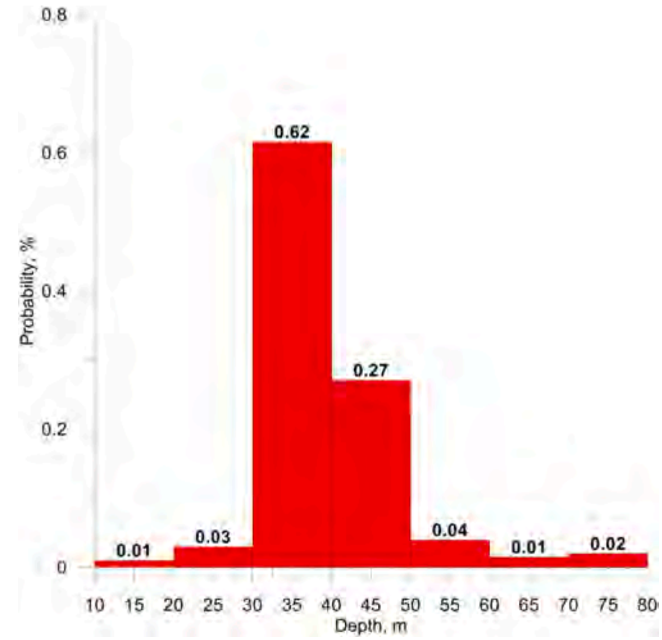

Fig. 3. Distribution of detected gas seepage along the bottom depth.

4.1.1. Spatial and temporal variability of the flares

The spatial and temporal variability of the seeps was studied at selected seepage by multiple hydroacoustic surveys on a hours- and days-scales. The observations of the seeps appearance showed that most seeps probably are temporally variable. Surveys conducted at Martyan seep site 15 and 23 November showed at Fig. 4 summarizes the positions of all flare areas detected during two time periods. Thus, at Martyan seep site 11 individual flares were recorded on November 15 and their number increased to 59 on November 23 (Fig. 4).

4.2. Gas flux

Based on acoustic survey data, estimates of gas flux were obtained for "clean" flares without acoustic noise from fish and jellyfish. A total of 26 recorded gas flare were processed at depths from 30.1 to 51.8 m (Table 2). To estimate the gas flow rate, the maximum value of acoustic backscattering in the bottom layer of water with a thickness h of 0.14 m was selected (h=tau*1446/2, tau = 0.2 ms). Several gas bubbles (1–3 pcs.) were recorded in the sample volume of the probing signal. This characteristic count of gas bubbles is confirmed by video frames of similar gas flares filmed in Laspi Bay, when 1–3 bubbles were

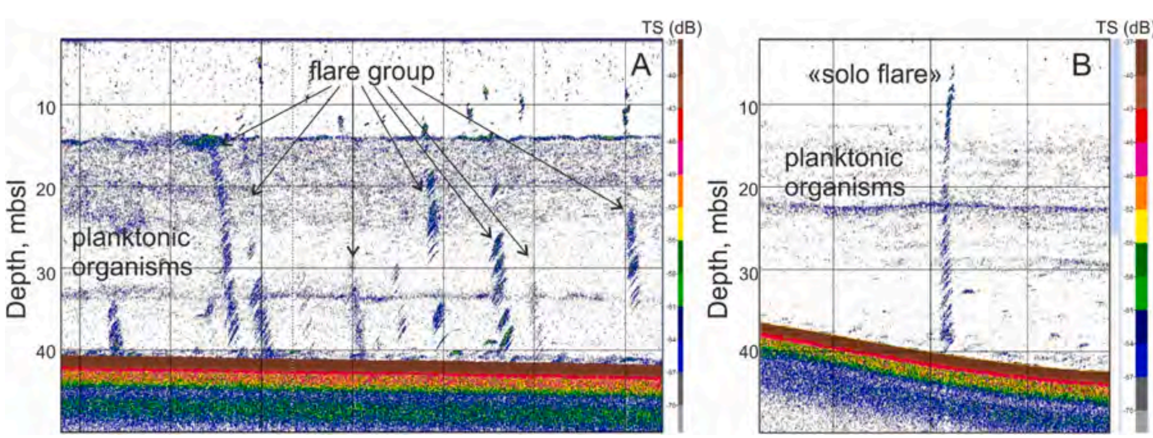

Fig. 2. Echograms (120 kHz), examples of acoustic recording of gas flares in the water area (A) - flare group at Martyan seep area and (B) individual flare at cape Plaka. The echograms were taken at a research vessel speed of 1,6 knots, echo sounder pulse duration 0.2 ms, echo integration threshold −80 dB.

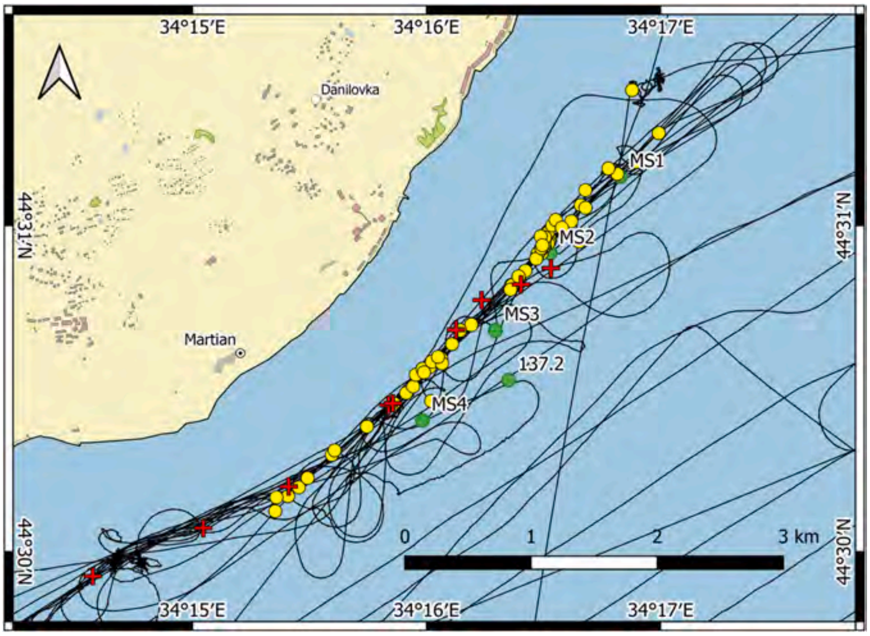

Fig. 4. Distribution of the flares detected within the Martyan seep area during two time periods: on November 15 (red crosses) and on November 23 2022 (yellow circles).

Table 2
Individual seep characteristics (depth and flare length) and corresponding gas flow rate.

Depth, m	Flare length,	mL·day^{-1}	mmol·s^{-1}	t·year^{-1}
43.62	15.01	65.17	0.147	0.074
43.97	22.97	79.13	0.179	0.090
44.21	19.51	88.60	0.200	0.101
39.29	23.12	85.42	0.193	0.097
42.77	14.68	27.70	0.063	0.032
40.94	31.58	33.60	0.069	0.035
43.12	31.22	4.50	0.008	0.004
43.55	13.62	34.16	0.056	0.028
42.70	36.46	56.33	0.121	0.061
40.28	35.05	12.52	0.020	0.010
41.91	22.44	4.07	0.008	0.004
44.26	19.44	24.50	0.052	0.026
42.41	17.02	10.73	0.023	0.011
40.14	15.19	22.05	0.029	0.015
40.17	22.58	40.69	0.081	0.041
42.98	17.45	24.40	0.044	0.022
37.80	33.80	33.96	0.061	0.031
46.52	26.80	86.23	0.198	0.100
46.95	31.35	15.74	0.031	0.016
30.87	6.47	23.32	0.036	0.018
39.86	10.36	49.35	0.106	0.054
51.77	12.62	32.82	0.080	0.040
42.98	17.87	18.80	0.036	0.018
39.72	17.45	45.52	0.091	0.046
37.45	23.12	62.46	0.116	0.059
39.01	29.93	6.57	0.013	0.006

simultaneously recorded in a single frame (Budnikov et al., 2019).

Calculated gas flow rates from individual flares ranged from 4.07 (0.04) to 88.6 (0.101) L·day^{-1} (t·year^{-1}), while the average value was 38 (0.07) L·day^{-1} (t·year^{-1}) (Table 2).

4.3. *Seafloor characteristics*

A Rovbuilder deployment was conducted at all flare sites in order to visually confirm the seafloor origin of the gas flares recorded hydroacoustically (Table 1), and the type of the surrounding sediments. During the all ROV-surveys gas bubble emissions were neither observed visually nor detected with the ROVmounted sonar. However, many times seeps were recorded at shallower depths by divers at the Martyan seep area 44°30′15, 34°14′02 (Fig. 5a) and Laspi seep area 44°25′15″, 33°42′25″ (Fig. 5b).

During the ROV dive at 'Laspi seep site" dense microbial mats, usually observed at active hydrocarbon-seeps, were observed. The sea floor was inspected along an approx. 500 m long track during 2,5 h. The sea floor was covered by decimeter-sized whitish material, occurring either as subcircular as elongated patches (Fig. 5c and d). These patches most probably represent microbial mats indicative of fluid flow from below. Any features of gas bubbles seepages as holes which could produced by bubbles emanating were not visible in the sea floor along the 'Laspi seep site" track. The sea floor at Cape Plaka seep site was covered with slightly elevated structures which formed topographic mounds up to a 10–15 cm high and 30–40 cm length (Fig. 5f). Whereas the sea floor at Martyan seep site was densely covered with clam shells (Fig. 5e).

4.4. *Oceanographic setting*

The hydrographic conditions at 4 seepage areas are shown in Fig. 6. In November 2022 the surface water consisted of about 40 m thick mixed layer below which a seasonal thermocline was found. At the investigated stations the water column had a temperature of 14–15 °C, a salinity of 18.6 – 18.7, a density of 13.4 kg m^{-3}, and oxygen concentrations of 6.7–6.8 mg·L^{-1}.

4.5. *CH_4 and He in sediments*

Vertical *ex situ* concentration profiles of methane dissolved in pore waters of shallow sediments were established for all stations investigated (Fig. 7, Tabl. 1). Methane was present in shallow sediments of all the research stations (Fig. 7). The highest concentration was measured in 139,1GC sediments – 0.7 mM. Generally, the concentrations increased with sediment depth at 104, 137.2, 135.1, 139, 139.1 stations (Fig. 7). At the other stations the values almost did not change with depth and even slightly decreased with depth at 136.2 (Fig. 7). The irregularities in the profiles were detected probably due to sediment decompression after core retrieval. Also, high concentrations of ethane were measured in the columns of two stations located in Laspi seep area

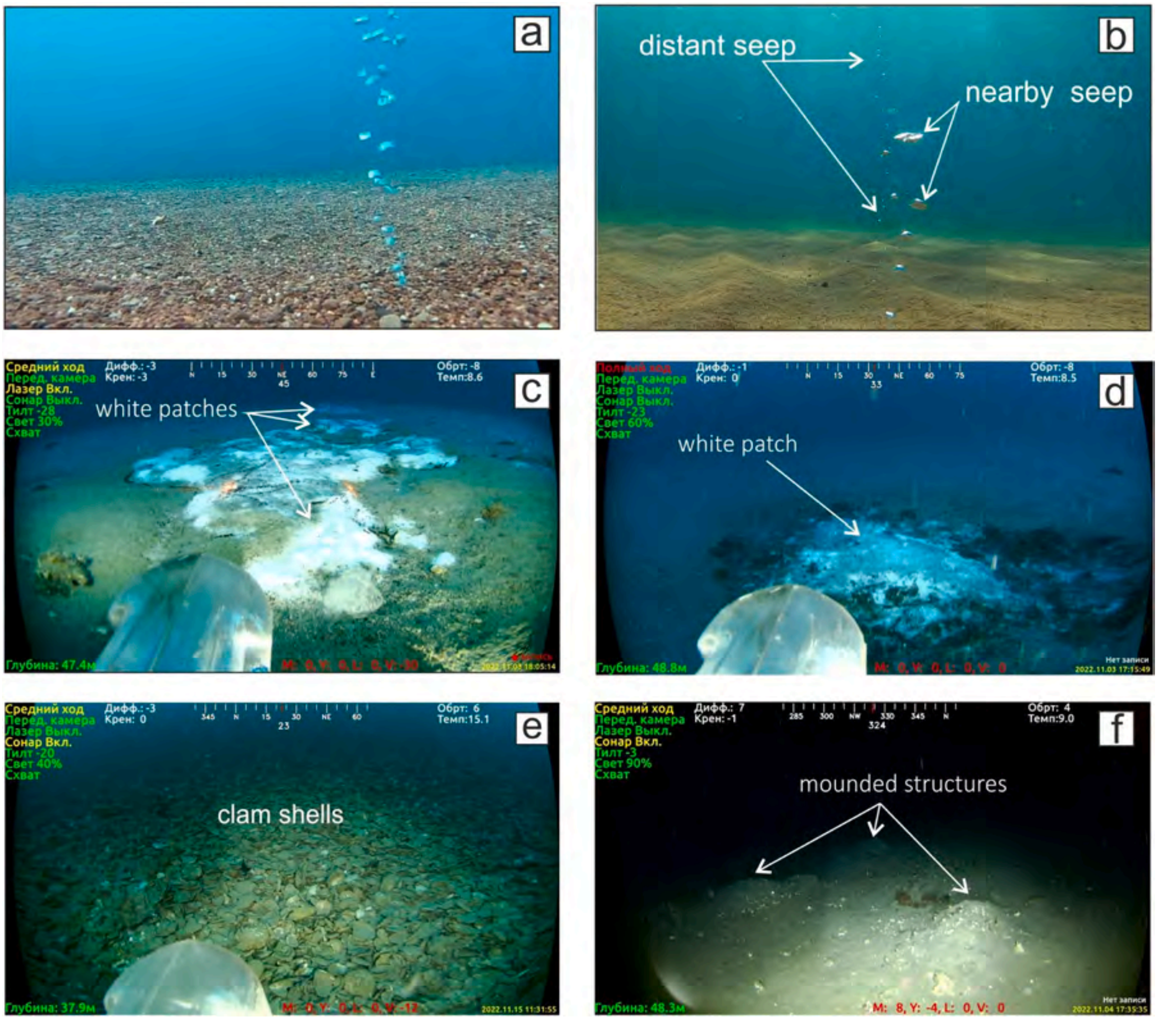

Fig. 5. Underwater pictures taken by divers at the very shallow sites of the Martyan seep area 44°30′15, 34°14′02 (a) and Laspi seep area 44°25′15″, 33°42′25″ (b) and showing gas bubbles and sandy floor (after Malakhova 2020), as well as sea floor picture taken with the high-resolution video camera mounted on the Rovbuilder RB 300 at Laspi Bay demonstrates the occurrence and intercalation of white colored patches (c, d); clams flaps at Martyan seep area (e); Cape Plaka seep area with elongated mounded structure (f). For locations see Fig. 1.

st.113 and Martyan seep area st. 137.2 up to 1 μM and 200 nM respectively.

The helium content along the sampled sediments averaged 10.7 parts per million (ppm). This value is considered the background level for the study area. For comparison, the background helium concentration in the sediments in the Tatar Strait (Sea of Japan) is 5.6 ppm and in the Kuril Basin (Sea of Okhotsk) is 4 ppm (Shakirov et al., 2016). The increased background of helium content in the sediments of the shallow shelf of Crimea may be associated with active tectonic activity in the area. Geological faults, mud volcanic activity, and hydrothermal vents are likely sources of helium. Additionally, the unique conditions of the Black Sea, including the lack of oxygen and difficulty with water exchange, create favorable conditions for helium accumulation in sediments (Greinert et al., 2006).

Significant results were obtained at stations 136.2-GC and Megaseep. Abnormally high helium concentrations were recorded at both locations, with 111,943 ppm (11.2 %) at station 136.2-GC at the 190-cm horizon and 4891 ppm (0.5 %) at the Megaseep site at the 100-cm horizon. These sites are located within the influence zone of an active fault, as identified by Sydorenko et al. (2017). It should be noted that these locations are also associated with active gas seeps and methane anomalies, as shown in Fig. 1.

4.6. *CH_4 in water*

The methane profiles above Martyan seep area show concentration decreases from higher concentrations (24 nM) close to the seafloor to low values between 5 and 10 nM close to the sea surface (Fig. 8). No perceptible change of the methane gradient was found for Laspi seep and Cape Plaka (Fig. 8). Using the mean atmospheric methane concentration of 1.9 ppm (Ocean Station M: http://www.esrl. noaa.gov/gmd/ccgg/iadv/, at 66.001 N, 2.001E) and the ambient T and S values (Fig. 6), the equilibrium methane concentration at the sea surface was estimated as 2.73 nM (after Wiesenburg, Guinasso Jr, 1979). Consequently, the measured mixed-layer methane concentrations between 4 and 15 nM indicate a saturation of 150–550 %.

4.7. *Determination of Hg concentration*

The sediment columns we studied can be divided into two groups – with mercury concentrations in the range of 8–45 ng g^{-1} and with mercury concentrations from 50 to 170 ng g^{-1} (Fig. 9). Higher mercury concentrations corresponded to the seep sites exceeding mercury concentrations in background areas by 2–3 times. The maximum concentration reached 170 ng g^{-1} in sediments of Laspi Bay (50 cm bbl, Fig. 9). This value did not exceed the standards for sediments according to the

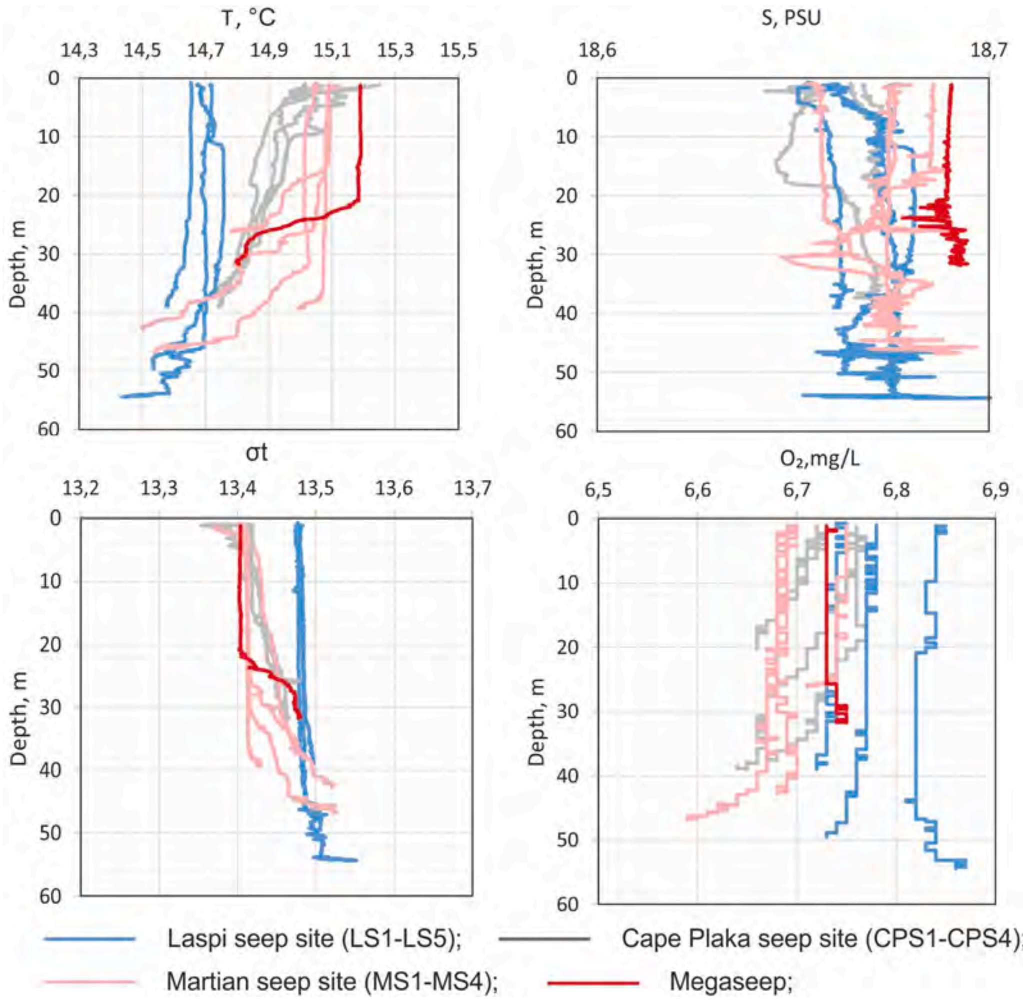

Fig. 6. Water column profiles of temperature (T), salinity (S), σt and dissolved oxygen (O_2), recorded in November 2022 at Laspi, Martyan, Cape Plaka and Megaseep areas.

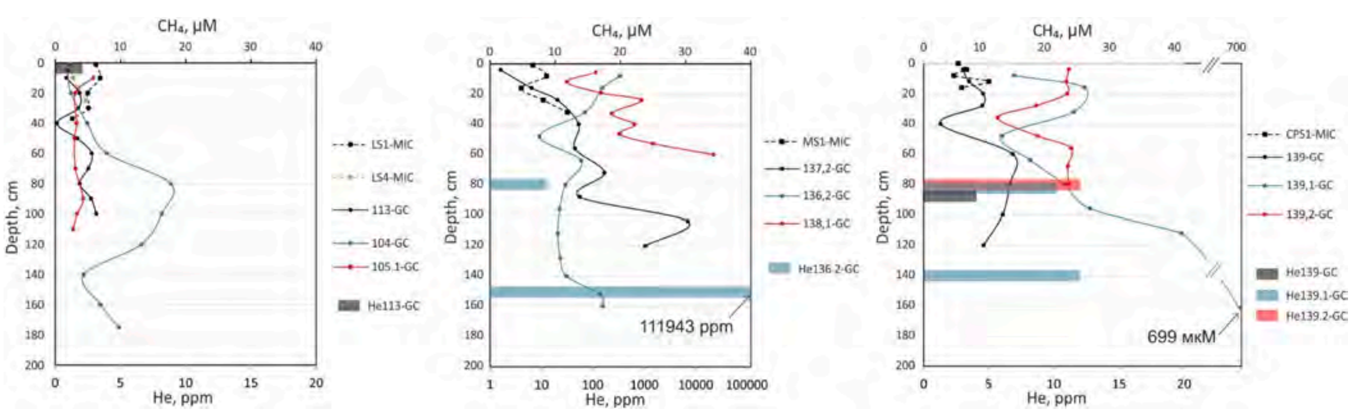

Fig. 7. Vertical concentration profiles of methane (lines) and helium (histograms) in sediments recovered. Numbers in legends indicate GC (solid lines) and MIC (dotted lines) cores.

"Dutch sheets" (300 ng g^{-1}) (Neue NiederlandischeListe, 3/95).

4.8. Hydrological parameters in the bottom layer at the Martyan gas emission site (November 15 and 23)

On November 15, 2023, measurements were taken from 12:30 p.m. to 2:30 p.m. local time (Fig. 10 left side). During the measurement period, changes in the bottom current velocity and direction were observed. During the period from 12:30 p.m. to 13:15 p.m. the north-eastern direction of the current prevailed, changing consistently to southeastern, southern and southwestern, and then again to north-eastern with flow about 15 cm/sec. The period from 13:15 p.m. to 14:00 p.m. was characterized by a rather stable current direction to the northwest with flow about 10 cm/sec. From 14:00 p.m. the flow

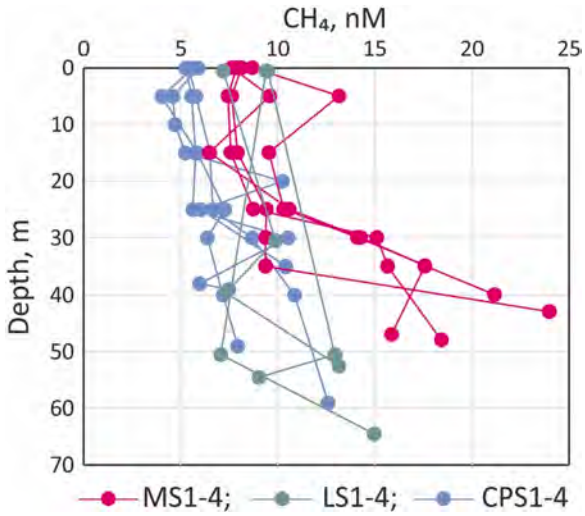

Fig. 8. Profiles of dissolved methane concentration for all CTD casts at seep areas.

significantly varied in direction from northward to southward in the sector 180–360° and in magnitude in the range from 3 to 34 cm/sec.

Changes in flow velocity and direction were concomitant with changes in turbidity. Between 12:30 p.m. and 13:05 p.m., turbidity varied between 2 and 4 NTU with an average of about 3 NTU. The period from 13:05 p.m. to 13:45 p.m. was characterized by more intense turbidity variations ranging from 3 to 9 NTU and an average of about 4 NTU. After 13:45 there was a decrease in turbidity to 2 NTU with small deviations from this value.

Salinity varied between 18.6 PSU and 18.8 PSU during the measurement. The temperature generally reduced from 14.9°C to 12.3°C until 14:00 p.m., then raised to 13.7°C from 14:00 p.m. to 14:15 p.m. and remained practically unchanged thereafter. Oxygen content up to 13:45 p.m. was 8.13 mg/l ± 0.08 mg/l and varied within the error of the sensor, however, starting at 13:45, there was first a decrease in oxygen concentration to 7.98 mg/l and then its rise to 8.16 mg/l.

On November 23, 2022, measurements were made from 18:10 p.m. to 18:40 p.m. local time (Fig. 10 right side). During the measurements, the flow velocity and direction did not change significantly. The flow was directed to the southeast, the value of the flow velocity was in the range of 5.3–10.3 cm/sec. Turbidity varied in the range of 1–3 NTU, no abrupt turbidity changes were observed. Salinity, as on November 15, 2022, ranged from 18.6 PSU to 18.8 PSU. The temperature remained constant within the sensor's accuracy and was approximately 13.85°C. The dissolved oxygen concentration DO was kept at 8.05 mg/L with a small peak at the beginning of the measurements to 8.13 mg/L, however, within the sensor's error range.

5. Discussion

We detected 204 hydroacoustic anomalies in the water column (gas flares) at the northern shelf of Crimea (Fig. 1, Table S1) during R/V Professor Vodianickiy cruise in November 2022. This new finding of methane seepage adds to the long and steadily growing list of seep areas in the world's oceans (Campbell, 2006; Judd and Hovland, 2009; Suess, 2014) and specifically in the Black Sea (Egorov et al., 2011).

The seeps are not randomly distributed, but are located over a depth range from 35 to 45 m (Fig. 4). Visual sea-floor inspections with the high-resolution video camera of the Rovbuilder system did not confirm active gas bubble emissions but detected white sea-bed patches at Laspi seep area as a marker of fluid release often accompanying methane gas emissions (Fig. 5c and 5d). Exploration of the seafloor at the base of water column bubble plumes sometimes fails to discover an active seafloor seep. This can be attributed to ephemerality of emissions, uncertainty in the seep's location, or extremely small size of the bubbles. Nonetheless, throughout this paper, we assume that identified water column plumes are indicative of seafloor gas seepage during the discrete time interval. Our data demonstrate that the flares are temporally variable over hours and weeks (4.4) and it is likely that the activity and intensity of the gas emissions may also change seasonally or annually.

5.1. *Intensity of gas seepage and comparison with other areas*

Our observations revealed that most imaged flares during our

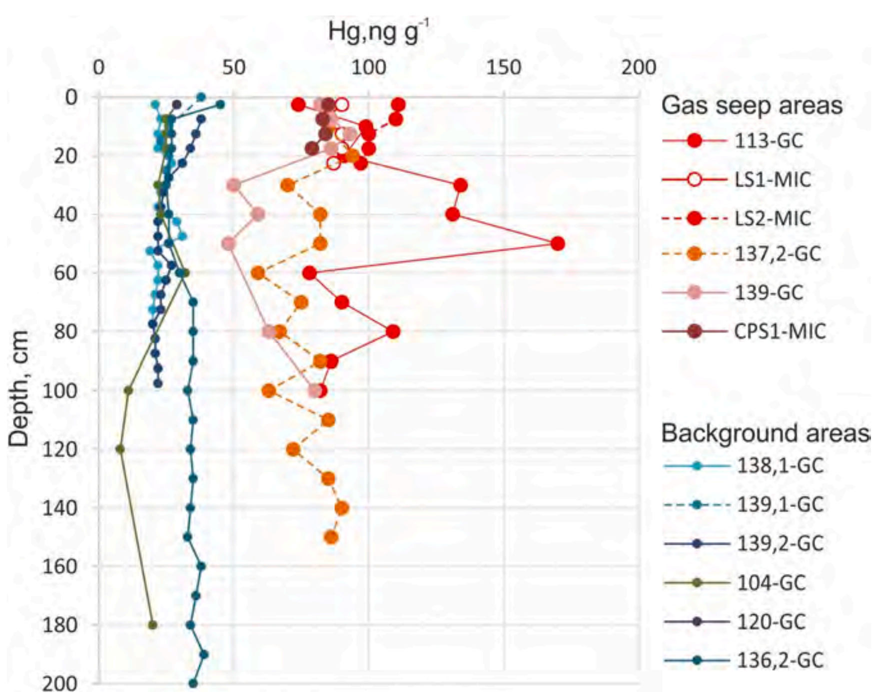

Fig. 9. Distribution of mercury in sediment columns at various stations (Note: GC – non-pressurized sediment cores recovered with gravity corers; MIC – mini corers).

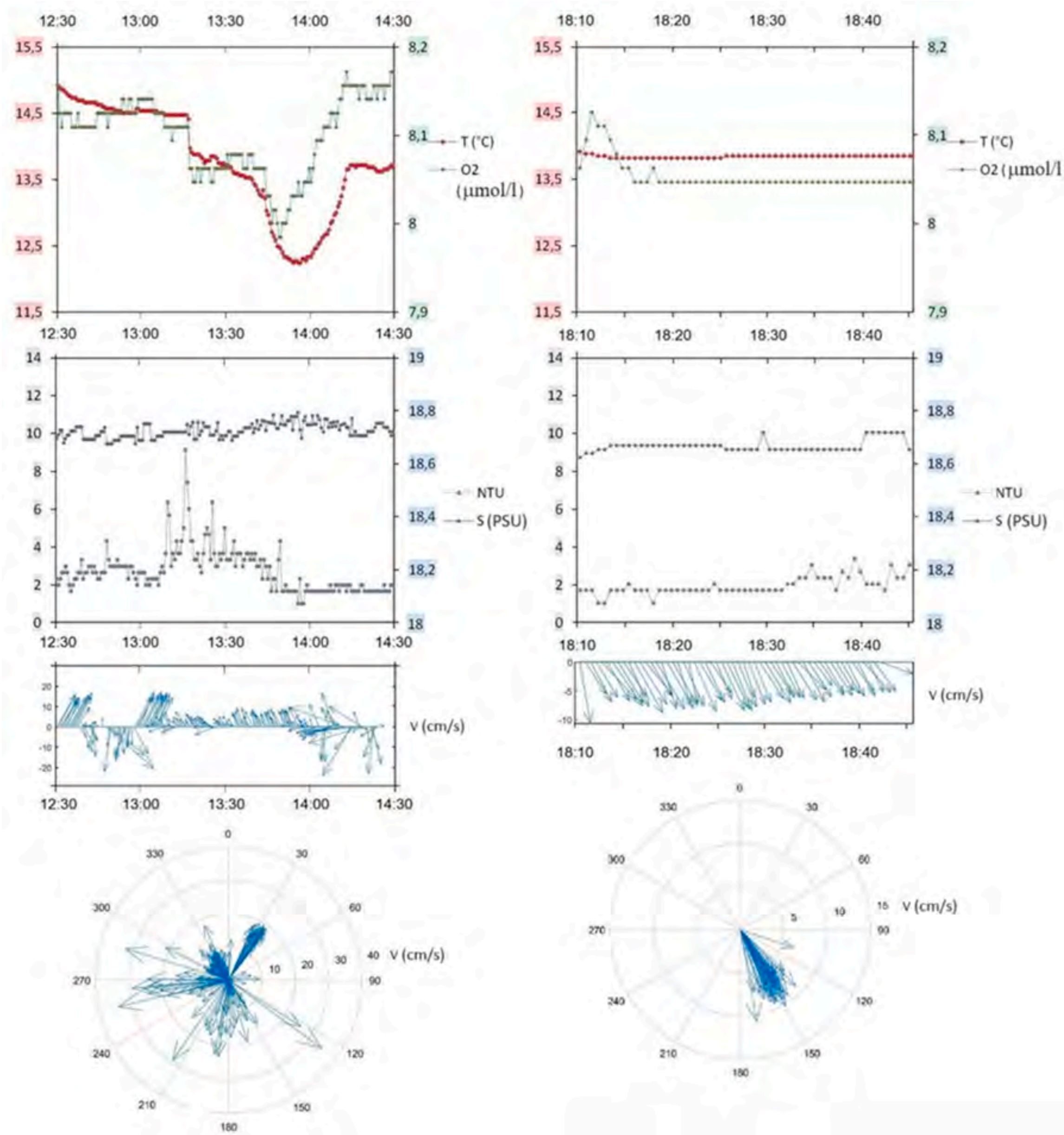

Fig. 10. Hydrological parameters in the bottom layer at the Martyan gas emission site at November 15 (left) and November 23 (right).

surveys are often appear episodically and are characterized by discharge in pulses. These data suggest that most of the flares are rather weak and represent discontinuous releases of gas bubble emissions. The quantity of bubbles and the intensity of seepage from the investigated area of Crimean continental margin seems to be rather weak in comparison to other well-researched seep areas in the Black Sea (Greinert et al., 2006, 2010; Naudts et al., 2006; Egorov et al., 2011; Römer et al., 2012), where vigorous gas bubble emissions and/or strong flares have been documented. Our estimates coincide with gas flow rates for very shallow seep site in Laspi Bay (Budnikov et al., 2019; Malakhova et al., 2024. Important to note that in Laspi Bay interseasonal observations performed in 2023 showed a relatively constant gas flow with yearly variations of no more than 30 % (Malakhova et al., 2024). Therefore, estimating the annual flux should account for a potential inaccuracy of 30 %. Meanwhile some biogenic sources may be inactive for months, which complicates annual extrapolations and necessitates more precise gas release statistics.

The estimates obtained for the average gas flux of individual flares (38 L·day^{-1}) allow us to evaluate the total flow from the entire water area of the southern coast of the Crimean peninsula. In this work 200 gas flares were fixed over an area of 7.1 km^2. Thus, the specific flux per square kilometer is 1070 L day^{-1} km^2. The estimated total gas flux from the shelf of the southern coast of Crimea, with an area of 10000 km^2, is about 10.7 10^3 m^3 of gas per day. This value is significantly less than the estimates made for the paleo-delta of the Dnieper, Danube and Don, where the average flux was 2.8 10^6 m^3 of gas per day (Artemov et al., 2019).

5.2. Fate of methane in the water column

The individual methane concentration profiles in Fig. 8 represent a snapshot of the local and likely time-dependent methane distribution patterns. The resulting profiles are strongly affected by currents and the proximity of the sampled water to rising gas bubbles, as well as dissolved methane transport from the bottom sediments to the water.

Our highest dissolved methane concentrations, measured in the bottom water during the all surveys (25 nM at Martyan seep area), are significantly lower in comparison to those observed at other shallow seep sites: in the Tommeliten, North Sea (268 nM; Schneider von Deimling et al., 2011), offshore Svalbard, west of Prins Karls Forland (524 nM; Gentz et al., 2014), seep field in central North Sea (1628 nM, Mau et al.,2015) and the Coal Oil Point seep field (up to 1900 nM; Mau et al., 2012). However, the CH_4 profiles at Martyan seep area still show elevated methane concentration in the bottom water and lower concentrations in the near surface layers at all 4 profiles (Fig. 8). We do not exclude that the near-bottom maxima can be a result of diffusion fluxes of dissolved gas. Sometimes such fluxes can be comparable or even exceed the bubble flux at the seep site (Malakhova et al., 2020, 2020). It is conceivable that our observations occurred in a period of minor seepage activity. For example, observations made for the Coal Oil Point seep field revealed interannual changes between 1990 and 2008, which have been related to internal geological processes (Bradley et al., 2010).

We assume that the hydrodynamic regime in the seepage area can impact the intensity of gas emissions as well as methane concentration in water column. Data obtained with RCM 9 LW showed that changes in the modulus and direction of current speed during measurements are coupled with changes in turbidity, temperature, and dissolved oxygen content. Atmospheric pressure fluctuations and surface waves can also affect the pulsations of gas bubble flow (Malakhova et al., 2024). Further research is needed to elucidate how seasonal variations in hydrophysical parameters of the water column affect the distribution of methane in the water column in the study area.

5.3. Genesis of bubble gas

We have discussed earlier genesis of bubble gas for some very shallow-water seeps of Crimean shelf compared to other Black Sea gas seepages areas (Malakhova et al., 2020). Our data revealed that gas bubble methane at the Heracles Peninsula seep sites as well as at Martyan seep area mainly originate from primary microbial path, the exception was Laspi Bay seeps which are thermogenic origin (Fig. 11). Single subbottom echosounder profiles presented by Khortov et al. (2023) indicate a domelike structure in shallow sediment depth interpreted as gas front. We assume that where this gas front comes very close to or even intercepts with the seafloor, gas ebullition is commonly observed.

5.4. Is mercury in bottom sediments a sign of gas discharge?

Geochemical studies indicate the presence of increased Hg concentrations in the water above mud volcanoes (Shnyukov et al., 1992; Sagalevich et al., 1992; Astakhov et al., 2011), hydrothermal formations (Torokhov and Taran, 1994; Astakhov et al., 2007) and at the areas of methane seeps (Egorov et al., 2003; Kostova et al., 2006; Ryzhov et al., 2003; Li et al., 2022). According to previous studies at the Black Sea (Kostova et al., 2006), the Hg concentration in the surface layer of bottom sediments from methane seeps area was about 7 times higher than at the background station and concentrations in the bottom water layer reached 2676 ng L^{-1}. Our data showed that Hg concentrations of sediments from gas seep-areas (87 ± 21 ng g, n = 49) are higher than those of background areas (26 ± 7 ng g-1, n = 91) especially in the near core-top layers (Fig. 9). Similar results were obtained for Haima cold seep (South China Sea, Li 2022). Total-Hg concentrations of seep sediments (65.27 ± 38.74 ng/g) were reliably higher than those of inactive-area (42.03 ± 3.15 ng g^{-1}). It has been shown that sedimentary organic matter is a crucial factor that influences the distribution and speciation Hg in marine sediments (Chakraborty et al.,2015) and the Hg/TOC values in sediments from the active seep area are higher compared to those from the inactive area and reference sites (Li et al., 2022). In future work, we aim to identify the Hg/TOC ratio used to assess the capacity of organic matter to adsorb mercury.

5.5. He in sediments

The presence of helium in the sediments of the Black Sea can be attributed to a unique combination of geological factors and characteristics of the region. Tectonic forces control the degassing zones in the Black Sea, and many land faults continue into the sea (Sheremet et al., 2016). Current gas emissions from the Crimean coast of the Black Sea are associated to seismic activity (Nikishin et al., 2015). Gas-geochemical analysis of sediment samples from the shallow water area reveals that gas release in this region has a deep origin. This release occurs in deep fault zones where tectonic activity is ongoing (Hippolyte et al., 2018). The high concentrations of helium and heavy hydrocarbons in bottom sediments indicate the deep nature of this degassing process (Shakirov et al., 2016; Syrbu et al., 2024).

The study of helium as an inert gas is useful for understanding the

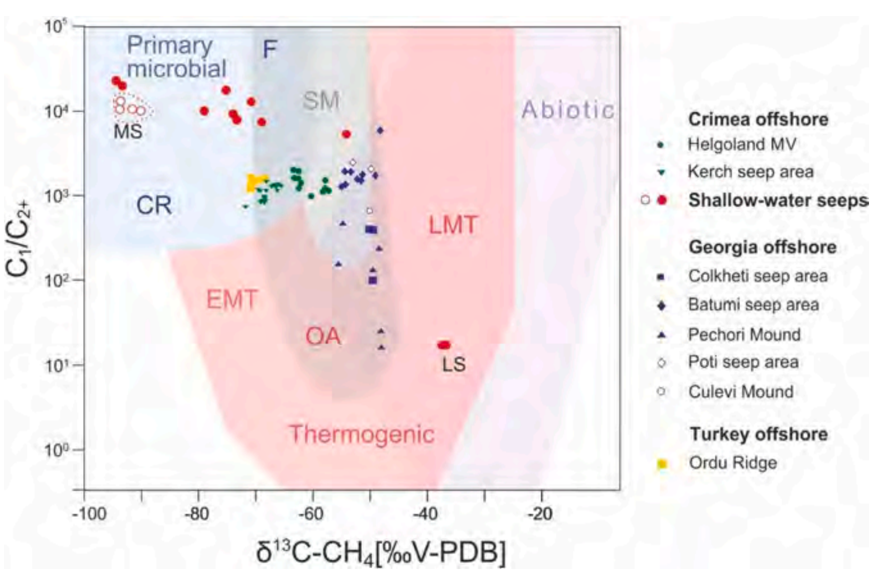

Fig. 11. Generic classifications of light hydrocarbons (adopted from Milkov and Etiope, 2018) illustrating hydrocarbon ratios (C_1/C_{2+}) vs. $\delta^{13}C$-CH_4 isotope data for the Crimea coastal areas and Black Sea gas samples from various sites (after Malakhova et al., 2020). LS – Laspi seep area; MS - Martyan seep area; CR – carbonate reduction, F – methyl-type fermentation, SM – secondary microbial, OA – oil-associated thermogenic gas, EMT – early mature thermogenic gas, LMT – late mature thermogenic gas.

nature of gas flows, as they are natural indicators that do not react chemically with the host rocks. Helium can be found in sediments and bottom waters, and it can be derived from three different sources with distinct isotopic signatures, allowing us to trace its origin and movement. These sources include the atmosphere, crust, and mantle Ballentine et al., 2002). For our study area, high concentrations of helium were recorded at stations 136.2-GC and Megaseep. In both cases, the helium anomalies suggest specific seepage processes occurring in the local area. These concentrations are likely characteristic of only this specific location, and they cannot indicate an increase in helium flow from the entire water area of the shallow Black Sea off the Crimean coast.This is confirmed by previous isotope studies of helium in this area (Sorokin trough) (Holzner et al., 2008). These studies confirmed that the helium in pore waters of sediment has a crustal origin with a small amount of mantle component, indicating a deep source for the helium.

Deep helium is likely to migrate along with natural gas (methane) through the bottom sediments. High concentrations of hydrocarbon gases, including helium, have previously been recorded in the sediments on the shelf off the coast of Crimea in the Black Sea (Shnyukov, 1992, 1998, 1999; Holzner et al., 2008). In the study by Holzner et al. (2008), helium concentrations were measured in pore waters, sediments, and water at a depth of 200 m in the Sorokin Trough, an area of active gas emission. It was found that helium concentrations increase with depth and reach their maximum in the bottom water layer, where it comes from the bottom sediments and accumulates, as vertical transport is slow. The study found that the bottom water layer is supersaturated with helium by approximately 20 % and the pore waters in the sediment core are 400 % supersaturated relative to the bottom layer. This confirms the influx of helium due to the advection of fluids through permeable zones in the Earth's crust, such as zones where active faults intersect.

5.6. Bacterial mats at Laspi Bay seep area

The presence of hydrogen sulfide, generated through sulfate reduction and discharged with fluids at bubble gas emissions sites, has been shown to stimulate the formation of bacterial biofilms/mats on the surface of sediments. Such mats have been documented many times for gas emissions along the coast of Crimea (Bryukhanov et al., 2018; Pimenov et al., 2018; Malakhova et al., 2023a, 2023b). These mats are predominantly composed of sulfur-oxidizing bacteria belonging to the genera Thiocapsa, Thiobaca, Thioflavicoccus, and Thiorhodococcus (Bryukhanov et al., 2018; Pimenov et al., 2018). But until now we did not register any biofilms in Laspi Bay shallow-water gas emission area (<4 m depth). Earlier we identified sulfur-oxidizing epsilonproteobacteria of the family Thiovulaceae (8.2 %) in the surface horizons of Laspi Bay sediments. Deeper (10–15 cm bsfl) archaea of the phylogenetic cluster ANME-2a/b (19.2 %) and bacteria of the family Desulfobacteraceae (12.2 %), mediating anaerobic methane oxidation, were detected (Malakhova 2020).

6. Conclusion and outlook

Our work is a piece in a larger puzzle dedicated to the study of methane seep areas in the world's oceans and specifically in the Black Sea. We have performed focused survey of gas bubble emissions at the Crimean continental margin (northern Black Sea) which has not been systematically surveyed before. During R/V Professor Vodianickiy 125/1 Cruise in November 2022 hydroacoustic and geochemical studies were carried out to detect gas seepage along coastline. More than 200 bubble-induced hydroacoustic anomalies in the water column (flares) were found at 7,1 km^2. This new finding of methane seepage adds to the long and steadily growing list of seep areas in the world's oceans (Judd and Hovland, 2009) and specifically in the Black Sea (Egorov et al., 2011). We allocated 4 seep clusters (Alupka, Martyan, Cape Plaka and Ribach'e) which are arranged in the west of the study area and included most of the identified hydroacoustic anomalies. The seeps were found to be temporally variable, with some showing episodic and discontinuous releases of gas bubbles. The quantity of bubbles and the intensity of seepage on the investigated area of Crimean continental margin seems to be rather weak in comparison to other well-researched seep areas in the Black Sea (Greinert et al., 2006, 2010; Naudts et al., 2006; Egorov et al., 2011; Römer et al., 2012), where vigorous gas bubble emissions and/or strong flares have been documented.

The gas flux from single localized gas seepage was calculated using the method of incoherent addition of the acoustic responses of an ensemble of gas bubbles and ranged from 4.07 (0.04) to 88.6 (0.101) L/d (t/y), average - 38 (0.07) L/d (t/y). The total gas flux of bubble methane from the seafloor at the surveyed area estimated by extrapolating was about 10.7 10^3 m^3 per day.

Our geochemical data (helium anomalies and high mercury concentrations in seep sediments) suggest a thermogenic origin for the gas, while previous isotopic data ($\delta^{13}C$) of bubble methane indicate a microbial origin with only one exception for Laspi Bay seep area. This discrepancy highlights the need for further research to clarify the nature of the emitted gas.

Research questions arising from our shallow gas seeps survey offshore Crimea include: 1) why the depth of gas emissions is limited to the 35–40 m isobath; 2) determining the factors leading to the high variability of seep activity on the synoptic scale; 3) assessing the role of thermogenic and biogenic gas contributions; 4) documenting the role of methane input on the local biocoenosis and associated biogeochemical processes.

Author statement

We, the authors, declare that this manuscript is original, has not been previously published, and is not under consideration for publication elsewhere. We confirm that all named authors have read and approved the manuscript, and no other individuals meet the authorship criteria who are not listed. Additionally, we confirm that the order of authors as listed has been approved by all. We understand that the corresponding author will serve as the primary contact for the editorial process and will be responsible for communication with co-authors regarding progress, submission of revisions, and final approval of proofs.

CRediT authorship contribution statement

Syrbu N. S.: Writing – original draft, Visualization, Methodology, Investigation, Formal analysis, Data curation. **Budnikov A. A.:** Writing – original draft, Validation, Formal analysis. **M.M. Makarov:** Visualization, Methodology, Investigation, Formal analysis, Conceptualization. **Malakhova Tatiana:** Writing – original draft, Visualization, Supervision, Project administration, Methodology, Investigation, Formal analysis, Data curation, Conceptualization. **A.P. Stetsiuk:** Writing – original draft, Methodology, Investigation, Formal analysis. **Khurchak A. I.:** Writing – original draft, Investigation, Formal analysis. **K.M. Kucher:** Methodology, Investigation, Formal analysis. **M.V. Ivanov:** Investigation, Formal analysis. **A.A. Legkodimov:** Validation, Investigation, Formal analysis.

Funding

This study was performed based on results of the 125/1 cruise of the R/V Professor Vodyanitsky (Centre of collective use "R/V Professor Vodyanitsky" of the A.O. Kovalevsky Institute of Biology of the Southern Seas of RAS). Sample processing, data analysis, and this manuscript writing were conducted in the framework of IBSS state research assignment "Study of biogeochemical patterns of radioecological and chemoecological processes in the ecosystems of water bodies of the Sea of Azov–Black Sea Basin in comparison with other areas of the World Ocean and individual aquatic ecosystems of their drainage basins to ensure sustainable development in the southern seas of Russia" (No.

124030100127–7) and as part of the State Programs for basic scientific research No: 124022100078–7 and the State Assignment of LIN SB RAS № 0279–2021–0004. Some sample processing was supported by RSCF grant 24–17–20030.

Declaration of Competing Interest

The authors declare the following financial interests/personal relationships which may be considered as potential competing interests: Malakhova Tatiana reports financial support was provided by Russian Sciense Foundation. If there are other authors, they declare that they have no known competing financial interests or personal relationships that could have appeared to influence the work reported in this paper.

Acknowledgements

We would like to express our gratitude for the excellent support by crews provided during the 125/1 Cruise R/V Professor Vodianickiy for their assistance during field work. We gratefully acknowledge V.V. Voitsekhovskaia (IBSS RAS), A. Zagovenkova, T.S. Yakimov (V.I. Il'ichev Pacific Oceanological Institute FEB RAS) for help during sampling.

Appendix A. Supporting information

Supplementary data associated with this article can be found in the online version at doi:10.1016/j.rsma.2025.104290.

Data availability

Data will be made available on request.

References

Amouroux, D., Roberts, G., Rapsomanikis, S., Andreae, M.O., 2002. Biogenic gas (CH4, N2O, DMS) emission to the atmosphere from near-shore and shelf waters of the north-western Black Sea. Estuar. Coast. Shelf Sci. 54 (3), 575–587.

Artemov, Y.G., Egorov, V.N., Gulin, S.B., 2019. Influx of streaming methane into anoxic waters of the Black Sea basin. Oceanology 59, 860–870. https://doi.org/10.1134/S0001437019060018.

Astakhov, A.S., Ivanov, M.V., Li, B.Y., 2011. Hydrochemical and atmochemical mercury dispersion zones over hydrothermal vents of the submarine Piip Volcano in the Bering Sea. Oceanology 51, 826–835. https://doi.org/10.1134/S0001437011050031.

Astakhov, A.S., Wallmann, K., Ivanov, M.V., Kolesov, G.M., Sattarova, V.V., 2007. Distribution and accumulation rate of Hg in the Upper Quaternary sediments of the Deryugin basin, Sea of Okhotsk. Geochem. Int. 45, 47–61. https://doi.org/10.1134/S0016702907010041.

Ballentine, C.J., Burgess, R., Marty, B., 2002. 13. Tracing Fluid Origin, Transport and Interaction in the Crust. Rev. Mineral. Geochem 47, 539–614.

Baumberger, T., Leifer, I., Scherwath, M., Joye, S., 2022. Recent advances in natural methane seep and gas hydrate systems. Front. Earth Sci. 10, 868609.

Bradley, E., Leifer, I., Roberts, D., 2010. Long-term monitoring of a marine geologic hydrocarbon source by a coastal air pollution station in Southern California. Atmos. Environ. 44 (38), 4973–4981.

Bryukhanov, A.L., Vlasova, M.A., Malakhova, T.V., Perevalova, A.A., Pimenov, N.V., 2018. Phylogenetic diversity of the sulfur cycle bacteria in the bottom sediments of the Chersonesus Bay. Microbiology 87, 372–381. https://doi.org/10.1134/S0026261718030025.

Budnikov, A.A., Malakhova, T.V., Ivanova, I.N., Linchenko, E.V., 2019. Application of a passive acoustic method for detection and estimation of shallow-water bubble gas emissions. Mosc. Univ. Phys. Bull. 74, 690–696. https://doi.org/10.3103/S0027134919060109.

Campbell, K.A., 2006. Hydrocarbon seep and hydrothermal vent paleoenvironments and paleontology: Past developments and future research directions. Palaeogeogr. Palaeoclimatol. Palaeoecol. 232 (2-4), 362–407. https://doi.org/10.1016/j.palaeo.2005.06.018.

Ceramicola, S., Dupré, S., Somoza, L., Woodside, J., 2018. Cold seep systems. Submar. Geomorphol. 367–387. https://doi.org/10.1007/978-3-319-57852-1_19.

Chakraborty, P., Sarkar, A., Vudamala, K., Naik, R., Nath, B.N., 2015. Organic matter—a key factor in controlling mercury distribution in estuarine sediment. Mar. Chem. 173, 302–309. https://doi.org/10.1016/j.marchem.2014.10.005.

Egorov, V.N., Artemov, Y.G., Gulin, S.B., 2011. Methane seeps in the black sea: environment-forming and ecological role. Sevastopol ECOSEA Hydrophys.

Egorov, V.M., Polikarpov, G.G., Gulin, S.B., Artemov, Ju.G., Stokozov, M.A., Kostova, S. K., 2003. Modern conception about forming-casting and ecological role of methane gas seeps from bottom of the Black Sea. Marin. Ecol. J. 2 (3), 5–26.

Gentz, T., Damm, E., von Deimling, J.S., Mau, S., McGinnis, D.F., Schlüter, M., 2014. A water column study of methane around gas flares located at the West Spitsbergen continental margin. Cont. Shelf Res. 72, 107–118. https://doi.org/10.1016/j.csr.2013.07.013, 2013. 2013.

Greinert, J., Artemov, Y., Egorov, V., De Batist, M., McGinnis, D., 2006. 1300-m-high rising bubbles from mud volcanoes at 2080 m in the Black Sea: hydroacoustic characteristics and temporal variability. Earth Planet. Sci. Lett. 244 (1-2), 1–15. https://doi.org/10.1016/j.epsl.2006.02.011.

Greinert, J., McGinnis, D.F., Naudts, L., Linke, P., De Batist, M., 2010. Atmospheric methane flux from bubbling seeps: spatially extrapolated quantification from a Black Sea shelf area. J. Geophys. Res. Oceans 115 (C1). https://doi.org/10.1029/2009JC005381.

Hillman, J.I., Klaucke, I., Bialas, J., Feldman, H., Drexler, T., Awwiller, D., Badhani, S., 2018. Gas migration pathways and slope failures in the Danube Fan, Black Sea. Mar. Pet. Geol. 92, 1069–1084. https://doi.org/10.1016/j.marpetgeo.2018.03.025.

Hippolyte, J.C., Murovskaya, A., Volfman, Y., Yegorova, T., Gintov, O., Kaymakci, N., Sangu, E., 2018. Age and geodynamic evolution of the Black Sea Basin: tectonic evidences of rifting in Crimea. Mar. Pet. Geol. 93, 298–314. https://doi.org/10.1016/j.marpetgeo.2018.03.009.

Holzner, C.P., McGinnis, D.F., Schubert, C.J., Kipfer, R., Imboden, D.M., 2008. Noble gas anomalies related to high-intensity methane gas seeps in the Black Sea. Earth Planet. Sci. Lett. 265 (3-4), 396–409. https://doi.org/10.1016/j.epsl.2007.10.029.

Ivanov, M.V., Pimenov, N.V., Rusanov, I.I., Lein, A.Y., 2002. Microbial processes of the methane cycle at the north-western shelf of the Black Sea. Estuar. Coast. Shelf Sci. 54 (3), 589–599.

Judd, A., Hovland, M., 2009. Seabed Fluid Flow: The Impact on Geology, Biology and the Marine Environment. Cambridge University Press. https://doi.org/10.1017/CBO9780511535918.

Khortov, A.V., Rimsky-Korsakov, N.A., Pronin, A.A., Mutovkin, A.D., 2023. Results of seismostratigraphic investigations of the crimean shelf by the method of continuous seismo-acoustic profiling. Dokl. Ross. Akad. Nauk. Nauk. o Zemle 512 (2), 295–301. https://doi.org/10.1002/0471914584.

Körber, J.H., Sahling, H., Pape, T., dos Santos Ferreira, C., MacDonald, I., Bohrmann, G., 2014. Natural oil seepage at kobuleti ridge, eastern Black Sea. Mar. Pet. Geol. 50, 68–82. https://doi.org/10.1016/j.marpetgeo.2013.11.007.

Kostova, S.K., Popovichev, V.N., Egorov, V.N., Plotitsyna, O.V., Artyomov, Yu.G., 2006. Distribution of mercury in water and bottom sediments in places of localization of jet methane gas emissions from the bottom of the Black Sea. Mar. Ecol. J. 5 (2), 47–56.

Kvenvolden, K.A., Rogers, B.W., 2005. Gaia's breath—Global methane exhalations. Mar. Pet. Geol. 22 (4), 579–590.

Lein, A., Yu, Ivanov, M.V., 2009. Biogeochemical Cycle of Methane in the. In: Ocean, A.P. (Ed.), Lisitsyn. Nauka, Moscow, p. 576 p.

Li, J., Dong, X., Tang, Y., Zhang, C., Yang, Y., Zhang, W., Peng, X., 2022). Deep sea cold seep is an atmospheric Hg sink and MeHg source.https://doi.org/10.21203/rs.3.rs-2323106/v1.

Makarov, M.M., Muyakshin, S.I., Kucher, K.M., Aslamov, I.A., Granin, N.G., 2020. A study of the gas seep Istok in the Selenga shoal using active acoustic, passive acoustic and optical methods. J. Gt. Lakes Res. 46 (1), 95–101. https://doi.org/10.1016/j.jglr.2019.10.014.

Malakhova, T.V., Budnikov, A.A., Ivanova, I.N., Murashova, A.I., 2020. Methane fluid discharge measurements by the trap method in Laspi Bay (Black Sea). Mosc. Univ. Phys. Bull. 75 (6), 705–711. https://doi.org/10.3103/S0027134920060132.

Malakhova, T.V., Budnikov, A.A., Ivanova, I.N., Khurchak, A.I., Khurchak, A.P., Krasnova, E.A., 2024. Passive acoustic monitoring for seabed bubble flows: case of shallow methane seeps at Laspi Bay (Black Sea). J. Acoust. Soc. Am. 156 (iss. 6), 4202–4216. https://doi.org/10.1121/10.0034605.

Malakhova, L.V., Egorov, V.N., Malakhova, T.V., Gulin, S.B., Artemov, Y.G., 2010. Methane in the Sevastopol coastal area, Black Sea. GeoMar. Lett. 30, 391–398.

Malakhova, T.V., Egorov, V.N., Malakhova, L.V., Artemov, Y.G., Pimenov, N.V., 2020. Biogeochemical characteristics of shallow methane seeps of Crimean coastal areas in comparison with deep-sea seeps of the Black Sea. Mar. Biol. J. 5 (4), 37–55. https://doi.org/10.21072/mbj.2020.05.4.04.

Malakhova, T.V., Malakhova, L.V., Murashova, A.I., Budnikov, A.A., Ivanova, I.N., Krasnova, E.A., 2023a. Monitoring of Shallow-Water Methane Seeps at Cape Fiolent (Black Sea). Oceanology 63 (1), 119–130. https://doi.org/10.1134/S0001437023010083.

Malakhova, T.V., Murashova, A.I., Ivanova, I.N., Budnikov, A.A., Malakhova, L.V., Krasnova, E.A., Pimenov, N.V., 2023b. Environment-forming effect of bubble gas emissions in the Golubaya Bay, Black Sea: oxygen regime and bacterial mats. Geochem. Int. 61 (3), 274–284. https://doi.org/10.1134/S0016702923030084.

Mau, S., Gentz, T., Körber, J.H., Torres, M.E., Römer, M., Sahling, H., Helmke, E., 2015. Seasonal methane accumulation and release from a gas emission site in the central North Sea. Biogeosciences 12 (18), 5261–5276. https://doi.org/10.5194/bg-12-5261-2015.

Mau, S., Heintz, M.B., Valentine, D.L., 2012. Quantification of CH4 loss and transport in dissolved plumes of the Santa Barbara Channel, California. Cont. Shelf Res. 32, 110–120. https://doi.org/10.1016/j.csr.2011.10.016.

McGinnis, D.F., Greinert, J., Artemov, Y., Beaubien, S.E., Wüest, A.N.D.A., 2006. Fate of rising methane bubbles in stratified waters: how much methane reaches the atmosphere? J. Geophys. Res. Oceans 111 (C9). https://doi.org/10.1029/2005JC003183.

Milkov, A.V., Etiope, G., 2018. Revised genetic diagrams for natural gases based on a global dataset of> 20,000 samples. Org. Geochem. 125, 109–120. https://doi.org/10.1016/j.orggeochem.2018.09.002.

Muyakshin, S.I., Sauter, E., 2010. The hydroacoustic method for the quantification of the gas flux from a submersed bubble plume. Oceanology 50, 995–1001. https://doi.org/10.1134/S0001437010060202.
Naudts, L., Greinert, J., Artemov, Y., Staelens, P., Poort, J., Van Rensbergen, P., De Batist, M., 2006. Geological and morphological setting of 2778 methane seeps in the Dnepr paleo-delta, Northwestern Black Sea. Mar. Geol. 227, 177–199.
Neue NiederlandischeListe // Altlasten Spektrum 3/95.
Nikishin, A.M., Okay, A.I., Tüysüz, O., Demirer, A., Amelin, N., Petrov, E., 2015. The Black Sea basins structure and history: New model based on new deep penetration regional seismic data. Part 1: Basins structure and fill. Mar. Pet. Geol. 59, 638–655. https://doi.org/10.1016/j.marpetgeo.2014.08.018.
Novikova, S.A., Shnyukov, Y.F., Sokol, E.V., Kozmenko, O.A., Semenova, D.V., Kutny, V. A., 2015. A methane-derived carbonate build-up at a cold seep on the Crimean slope, north-western Black Sea. Mar. Geol. 363, 160–173.
Obzhirov, A.I., 1993. Gas-geochemical fields of the bottom layer of seas and oceans. Sci. Publ.
Özel, Ö., Dondurur, D., Klaucke, I., 2022. Seismic and geoacoustic evidence for subsurface fluid flow and seepage offshore Akçakoca, Southwestern Black Sea, Turkey. GeoMar. Lett. 42 (4), 17. https://doi.org/10.1007/s00367-022-00740-z.
Pape, T., Bahr, A., Klapp, S.A., Abegg, F., Bohrmann, G., 2011. High-intensity gas seepage causes rafting of shallow gas hydrates in the southeastern Black Sea. Earth Planet. Sci. Lett. 307 (1-2), 35–46.
Pape, T., Blumenberg, M., Reitz, A., Scheeder, G., Schmidt, M., Haeckel, M., Blinova, V. N., Ivanov, M.K., Sahling, H., Wallmann, K., Bohrmann, G., 2021. Oil and gas seepage offshore Georgia (Black Sea)–Geochemical evidences for a Paleogene-Neogene hydrocarbon source rock. Mar. Pet. Geol. 128, 104995.
Pimenov, N.V., Merkel, A.Y., Tarnovetskii, I.Y., Malakhova, T.V., Samylina, O.S., Kanapatskii, T.A., Vlasova, M.A., 2018. Structure of microbial mats in the Mramornaya Bay (Crimea) coastal areas. Microbiology 87, 681–691. https://doi.org/10.1134/S0026261718050132.
Reeburgh, W.S., 2007. Oceanic methane biogeochemistry. Chem. Rev. 107 (2), 486–513. https://doi.org/10.1021/cr050362v.
Riedel, M., Hähnel, L., Bialas, J., Bachmann, A.K., Gaide, S., Wintersteller, P., Bohrmann, G., 2021. Controls on gas emission distribution on the continental slope of the western Black Sea. Front. Earth Sci. 8, 601254. https://doi.org/10.3389/feart.2020.601254.
Römer, M., Sahling, H., Pape, T., Bahr, A., Feseker, T., Wintersteller, P., Bohrmann, G., 2012. Geological control and magnitude of methane ebullition from a high-flux seep area in the Black Sea—the Kerch seep area. Mar. Geol. 319, 57–74. https://doi.org/10.1016/j.margeo.2012.07.005.
Ryzhov, V.V., Mashyanov, N.R., Ozerova, N.A., Pogarev, S.E., 2003. Regular variations of the mercury concentration in natural gas. Sci. Total Environ. 304 (1-3), 145–152. https://doi.org/10.1016/S0048-9697(02)00564-8.
Sagalevich, A.M., Torokhov, P.V., Matveyenkov, V.V., Galkin, S.V., Moskalev, L.I., 1992. Hydrothermal manifestations at Piyp submarine volcano, Bering Sea. Int. Geol. Rev. 34 (12), 1200–1209. https://doi.org/10.1080/00206819209465662.
Saunois, M., Stavert, A.R., Poulter, B., et al., 2020. The global methane budget. Earth Syst. Sci. Data Discuss. 12, 1561–1623.
Schmale, O., Beaubien, S.E., Rehder, G., Greinert, J., Lombardi, S., 2010. Gas seepage in the Dnepr paleo-delta area (NW-Black Sea) and its regional impact on the water column methane cycle. J. Mar. Syst. 80 (1-2), 90–100. https://doi.org/10.1016/j.jmarsys.2009.10.003.
Schmale, O., Greinert, J., Rehder, G., 2005. Methane emission from high-intensity marine gas seeps in the Black Sea into the atmosphere. Geophys. Res. Lett. 32 (7). https://doi.org/10.1029/2004GL021138.
Shakirov, R.B., Syrbu, N.S., Obzhirov, A.I., 2016. Distribution of helium and hydrogen in sediments and water on the Sakhalin slope. Lithol. Miner. Resour. 51, 61–73. https://doi.org/10.1134/S0024490216010065.
Sheremet, Y., Sosson, M., Ratzov, G., Sydorenko, G., Voitsitskiy, Z., Yegorova, T., Murovskaya, A., 2016. An offshore-onland transect across the north-eastern Black Sea basin (Crimean margin): Evidence of Paleocene to Pliocene two-stage compression. Tectonophysics 688, 84–100. https://doi.org/10.1016/j.tecto.2016.09.015.
Shnyukov E.F.. Mud volcanism in the Black Sea // Geol. zhurnal - 1999. - no. 2. - C. 38-47. *(in Russian)*.
Shnyukov, E.F., Gnatenko, G.I., Nesterovskii, V.A., Gnatenko, O.V., 1992. Mud volcanism of the Kerch-Taman region. Kyiv Nauk. Dumka.
Shnyukov, E.F., Ziborov, A.P., 2004. Mineral resources of the Black Sea. Kiev 277.
Starostenko, V.I., Rusakov, O.M., Shnyukov, E.F., Kobolev, V.P. and Kutas, R.I., 2010. Methane in the northern Black Sea: characterization of its geomorphological and geological environments.
Suess, E., 2014. Marine cold seeps and their manifestations: geological control, biogeochemical criteria and environmental conditions. Int. J. Earth Sci. 103, 1889–1916. https://doi.org/10.1007/s00531-014-1010-0.
Sydorenko, G., Stephenson, R., Yegorova, T., Starostenko, V., Tolkunov, A., Janik, T., Omelchenko, V., 2017. Geological structure of the northern part of the Eastern Black Sea from regional seismic reflection data including the DOBRE-2 CDP profile. Geol. Soc. Lond. Spec. Publ. 428 (1), 307–321. https://doi.org/10.1144/SP428.15.
Syrbu, N., Kholmogorov, A., Stepochkin, I., Lobanov, V., Shkorba, S., 2024. Formation of Abnormal Gas-Geochemical Fields and Dissolved Gases Transport at the Shallow Northeastern Shelf of Sakhalin Island in Warm Season: Expedition Data and Remote Sensing. Water 16 (10), 1434.
Tarnovetskii, I.Y., Merkel, A.Y., Kanapatskiy, T.A., Ivanova, E.A., Gulin, M.B., Toshchakov, S., Pimenov, N.V., 2018. Decoupling between sulfate reduction and the anaerobic oxidation of methane in the shallow methane seep of the Black Sea. fny235 FEMS Microbiol. Lett. 365 (21). https://doi.org/10.1093/femsle/fny235.
Torokhov, P.V., Taran, Y.A., 1994. Hydrothermal fields of the Piip submarine volcano, Komandorsky Back-Arc Basin: Chemistry and origin of vent mineralization and bubbling gas. Bull. Geol. Soc. Den. 41 (1), 55–64.
Veloso, M., Greinert, J., Mienert, J., De Batist, M., 2015. A new methodology for quantifying bubble flow rates in deep water using splitbeam echosounders: examples from the A rctic offshore NW-S valbard. Limnol. Oceanogr. Methods 13 (6), 267–287. https://doi.org/10.1002/lom3.10024.
von Deimling, J.S., Rehder, G., Greinert, J., McGinnnis, D.F., Boetius, A., Linke, P., 2011. Quantification of seep-related methane gas emissions at Tommeliten, North Sea. Cont. Shelf Res. 31 (7-8), 867–878. https://doi.org/10.1016/j.csr.2011.02.012.
Weber, T., Wiseman, N.A., Kock, A., 2019. Global ocean methane emissions dominated by shallow coastal waters. Nat. Commun. 10 (1), 4584. https://doi.org/10.1038/s41467-019-12541-7.
Wiesenburg, D.A., Guinasso Jr, N.L., 1979. Equilibrium solubilities of methane, carbon monoxide, and hydrogen in water and sea water. J. Chem. Eng. data 24 (4), 356–360. https://doi.org/10.1021/je60083a006.
Zori, A.A., Korneev, V.D., Khlamov, M.G., 2000. Methods means systems for measurement and control of parameters of marine vehicles. Donetsk RIA DSTU *388*.